J Incl Phenom Macrocycl Chem (2009) 64:305–315
DOI 10.1007/s10847-009-9569-y

ORIGINAL ARTICLE

# Dipyridamole/β-cyclodextrin complexation: effect of buffer species, thermodynamics, and guest–host interactions probed by $^1$H-NMR and molecular modeling studies

**Mahmoud M. Al Omari · Musa I. El-Barghouthi · Mohammad B. Zughul · J. Eric D. Davies · Adnan A. Badwan**

Received: 30 December 2008 / Accepted: 12 March 2009 / Published online: 27 March 2009


**Abstract** The complexation parameters of dipyridamole (Dipy) with β-cyclodextrin (β-CD) were investigated by using several techniques including phase solubility diagrams (PSD), proton nuclear magnetic resonance ($^1$H-NMR), x-ray powder diffractometry (XRPD), differential scanning calorimetry (DSC), scanning electron microscopy (SEM) and molecular mechanical modeling ($MM^+$). From the pH-solubility profiles, two basic p$K_a$s at 6.4 and 2.7 were estimated. The linear correlation of the free energy of Dipy/β-CD complex formation ($\Delta G_{11}$) with the corresponding free energy of inherent Dipy aqueous solubility ($\Delta G_{So}$), obtained from the linear variation of ln $K_{11}$ with that of the inherent Dipy solubility (ln $S_o$) at different pHs and ionic strengths, was used to measure the contribution of the hydrophobic character of Dipy to include into the hydrophobic β-CD cavity. Complex formation of Dipy was driven by favorable enthalpy ($\Delta H° = -14.8$ kJ/mol) and entropy ($\Delta S° = 31.9$ J/mol K) factors. $^1$H-NMR and molecular mechanical modeling studies indicate the formation of different isomeric 1:1 and 1:2 complexes, where both the piperidine and diethanolamine moieties get separately included into the β-CD cavity. Molecular mechanical modeling computations indicate that the dominant driving force for complexation is Van der Waals with lower contribution from electrostatic interactions. $^1$H-NMR and XRPD, DSC, SEM studies of isolated solid complexes indicate the formation of inclusion complexes in aqueous solution.

**Keywords** Dipyridamole · β-Cyclodextrin · Hydrophobic effect · $^1$H-NMR · Thermodynamic · Complex characterization · Molecular modeling

M. M. Al Omari (✉) · A. A. Badwan
The Jordanian Pharmaceutical Manufacturing Company, Um Al-Amad, Jordan
e-mail: momari@jpm.com.jo

M. I. El-Barghouthi
Department of Chemistry, The Hashemite University, Zarqa, Jordan

M. B. Zughul
Department of Chemistry, University of Jordan, Amman, Jordan

J. E. D. Davies
Department of Environmental Science, Lancaster University, Lancaster, England, UK

## Introduction

Dipy is 2, 2′, 2″, 2‴- [(4,8-dipieridinopyrimide [5,4-*d*] pyrimidine-2,6-diyl) dinitrilo] tetraethanol (Fig. 1). It is used as a non-nitrate coronary vasodilator. It is available under the brand names Persantine® tablets (25, 50, and 75 mg) and Aggrenox® capsules (200 mg extended-release in combination with 25 mg immediate-release aspirin) for Boehringer Ingelheim/Germany. Also it is available as a parenteral injection (5 mg/mL) for Abraxis, Apotex, Baxter, Bedford, Hospira and Sicor. It has a partition coefficient (LogP) of 1.5 with a relatively low oral bioavailability (37–66%) [1, 2].

Dipy occurs as an intensely yellow, crystalline powder or needless with a bitter taste. It is practically insoluble in water, very soluble in methanol, ethanol and chloroform, and practically insoluble in ether. It melts at 166.3 °C with an enthalpy of fusion equal to 4.4 J/g as measured by DSC [1, 3].

Cyclodextrins have been used to enhance the solubility of water-insoluble drugs through the formation of more soluble inclusion complexes in aqueous solutions and

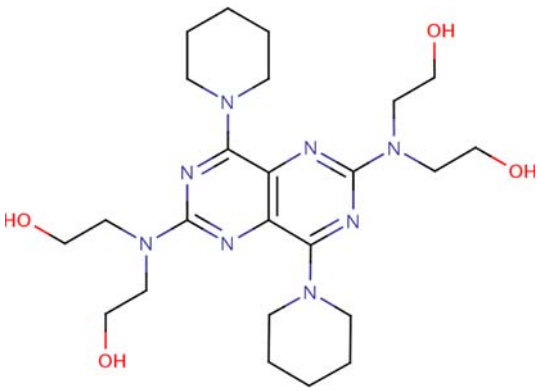


**Fig. 1** Molecular structure of dipyridamole

subsequently led to improve the pharmacokinetic parameters and to reduce the dosage of the drug with consequent advantages from an economic and toxicological point of view [4–6].

Interaction of cyclodextrins with Dipy was studied [7]. The phase solubility and $^1$H-NMR analysis indicated that $\beta$-CD was most suitable for inclusion compared with $\alpha$-and $\gamma$-CD. This was related to a better size fit to the $\beta$-CD internal hydrophobic cavity. The study also indicated that the presence of $\beta$-CD improves the stability to Dipy.

However, guest–host interactions of Dipy with $\beta$-CD involving inclusion complex characterization have not yet been reported. In this work, the effect of pH of solution and temperature on the interaction of Dipy with $\beta$-CD were studied. A quantitative estimate of the contribution of the hydrophobic character of Dipy and specific interactions to complex stability with $\beta$-CD was determined from the linear dependence of the free energy of 1:1 complex formation ($-$RT ln $K_{11}$) on that of the inherent Dipy solubility ($S_o$), obtained at different pHs, buffer type and buffer concentrations. The thermodynamic parameters were also estimated to evaluate the driving forces for complex formation. In addition, XRPD, DSC, SEM, $^1$H-NMR and MM+ studies were carried out to verify inclusion complex formation, and to explore guest–host interaction sites.

## Materials and methods

### Materials

Dipyridamole (99%) from S·I.M.S. (Italy) and $\beta$-CD (101.0%) from Wacker Chemie (Germany) were provided by The Jordanian Pharmaceutical Manufacturing Company (JPM). The hydrochloride salt of Dipy and its $\beta$-CD complex were prepared by dissolving a mixture of Dipy with $\beta$-CD (1 mmol:2 mmol) in sufficient amount of aqueous containing HCl (2 mmol). The samples were freeze-dried (FD3, Heto-Holten A/S, Denmark) and the solids were collected. Aqueous solutions of $\beta$-CD (12 mM) and Dipy HCl (2 mM) were separately freeze-dried and the obtained solids were used to prepare the physical mixture for comparison in the XRPD, DSC, and SEM studies. All other chemicals were of analytical grade obtained from Merck (Germany) and Surechem (UK).

### Acid–base ionization constant (p$K_a$) and solubility products (p$K_{sp}$s) determination

#### *By UV/visible spectrophotometry*

A stock solution of Dipy (1.0 mM each) was prepared by dissolving 0.1 mmole in 100 mL of methanol, which was diluted further with 0.05 M citrate buffers of different pHs ranging from 2 to 12 to obtain final solutions having fixed concentration of 0.02 mM. The pH of solution was adjusted by NaOH solution to obtain the desired pH. The absorbances of these solutions were measured at 30 °C using first derivative UV/visible spectrophotometry at 294 nm. It should be noted that first derivative UV spectrophotometry was consistently used throughout this work following careful examination of absorption spectra against $\beta$-CD concentration at different pHs, which offered the maximum differences in absorbance.

The p$K_a$s of Dipy was determined using the acid–base equilibrium shown below and following the procedure discussed earlier [8].

$$BH^+ \rightleftharpoons H^+ + B; K_{a1} = \frac{(H^+)[\mathrm{B}]}{y[\mathrm{BH}^+]} \quad (1)$$

$$BH_2^{2+} \rightleftharpoons H^+ + BH^+; K_{a2} = \frac{(H^+)y[\mathrm{BH}^+]}{y^4[\mathrm{BH}_2^{2+}]} \quad (2)$$

Nonlinear regression of the measured absorbance ($A$) against pH, with the molar absorptivities ($\varepsilon$) and $K_a$ used as floating parameters, yields the best estimates of $K_a$, by minimizing the function SSE $= \sum (A^P - A)^2$ where

$$\begin{aligned} A^P &= \{\varepsilon_B[\mathrm{B}] + \varepsilon_{BH^+}[\mathrm{BH}^+] + \varepsilon_{BH_2^{2+}}[\mathrm{BH}^{2+}]\} \\ &= C\{\varepsilon_B f_B + \varepsilon_{BH^+} f_{BH^+} + \varepsilon_{BH_2^{2+}} f_{BH_2^{2+}}\} \end{aligned} \quad (3)$$

while $\varepsilon_B$, $\varepsilon_{BH^+}$ and $\varepsilon_{BH_2^{2+}}$ are the molar absorptivities of $B$, $BH^+$ and $BH_2^{2+}$, respectively, $C$ is the molar concentration of Dipy, which was kept constant at 0.02 mM, and $f_B$, $f_{BH^+}$ and $f_{BH_2^{2+}}$ are the fractions of $B$, $BH^+$ and $BH_2^{2+}$ present in solution at each pH.

#### *By pH solubility profile*

Excess amounts of Dipy (500 mg) were added to 50 mL of 0.05 M citrate buffers of different pHs ranging from 3.0 to 9.5. The samples were mechanically shaken in a thermostatic bath shaker (1086, GFL/Germany) at 30 °C to attain

equilibrium; an aliquot was filtered using a 0.45 μm filter (cellulose acetate or cellulose nitrate, Advantec MFS Inc., Duplin, USA). The pH of the filtrate was measured by a calibrated pH-meter (3030, Jenway/England). The Dipy content was measured using 1st derivative spectrophotometry at 278 nm.

Referring to the acid/base equilibria of Dipy indicated in Eqs. 1 and 2 above, estimates of the ionization constants ($pK_a s$) of Dipy and the solubility product ($pK_{sp}$) of the corresponding citrate salt were obtained by nonlinear regression of the measured inherent solubility ($S_o$) of Dipy against pH as shown below and following the procedure discussed earlier [8, 9].

$$S_o^P = [B] + [BH^+] + [BH_2^{2+}] = [BH^+]\left\{1 + \frac{yK_{a1}}{(H^+)} + \frac{(H^+)}{y^3 K_{a2}}\right\} \quad (4)$$

or

$$S_o^P = [BH^+]\left\{1 + \frac{yK_{a1}}{(H^+)}\right\} + \frac{K_{sp12}}{y^6[X^-]^2} \quad (5)$$

where $X^-$ denotes the citrate$^-$ ion species, and $K_{sp}$ is the solubility product of the salt given by

$$(BH_2^{2+})X_2^{2-}(s) \rightleftharpoons BH^{2+} + 2X^-; K_{sp12} = y^6[BH_2^{2+}][X^-]^2 \quad (6)$$

Equation 4 is automatically switched into Eq. 5 in the pH region if $S_o$ is limited by saturation of the (Dipy.$H_2^{2+}$)(citrate$^-$)$_2$ salt (pH < 5) where $B$, $BH^+$, and $BH_2^{2+}$ denote neutral, monoprotonated and diprotonated Dipy, respectively. $(H^+) = 10^{-pH}$ and $y$ is the molar mean activity coefficient of ionic species given by the Davies equation: $\log\ y_i = -B\ |z^+ z^-|\ \{\sqrt{I}/(1+\sqrt{I}) - 0.3\ I\}$, where $I = -½ \sum c_i z_i^2$ and $B = 1.825 \times 10^6\ \rho^{1/2}/(\varepsilon T)^{3/2}$ while $\rho$ and $\varepsilon$ are respectively the density and dielectric constant of water at absolute temperature $T$. Best estimates for $pK_a$, and $pK_{sp}$ values were obtained by minimizing the function SSE $= \sum (S_o{}^P - S_o)^2$ where $S_o$ is the inherent solubility of Dipy and $S_o{}^P$ is the predicted value of $S_o$.

## Stability of dipyridamole solution in the absence and presence of β-CD

A total of 20 mL portions of the Dipy methanolic solution (1.25 mM) were separately transferred into 100 mL volumetric flasks, diluted to 100 mL with 0.05 M citrate buffers (pHs 4.0 and 9.0) to obtain solutions having concentration of 0.25 mM. The final solutions were incubated at 45 °C (HC 0020 incubator, Heraeus Vötsch/Germany) for 2 days. The same procedure was repeated but 0.022 mmole of β-CD was added to the volumetric flasks prior to final dilution. The samples before and after incubation were then diluted to their half concentration by methanol and analyzed using the HPLC method [7]. HPLC instrument equipped with a P1000 pump and a UV1000 detector (TSP/USA). A mixture of methanol and aqueous solution containing 0.005 M sodium heptane sulfonate and 0.1% of acetic acid (80:20 v/v) was used as the mobile phase and octyl silane column as the stationary phase (BDS Hypersil C8 150 × 4.6 mm, 5 μm). The UV detector was set at 254 nm, a flow rate of 1.0 mL/min and an injection loop of 20 μL were used.

## Phase solubility studies

Solubility studies were performed as described earlier by Higuchi and Connors [10]. Excess amounts of Dipy (200 mg) were added to 50 mL of buffered aqueous β-CD solutions ranging in concentration from 0 to 18 mM. The solutions include: citrate and phosphate buffers of different pHs (ranging from 4.1 to 10.5) and different concentrations (ranging from 0.05 to 2.0 M). The samples were mechanically shaken in a thermostatic bath shaker (1086, GFL/Germany) at 30 °C. The content of Dipy was measured at different time intervals of thermostatic mechanical shaking to reach equilibrium and to ascertain that not supersaturation is taking place. A period of 2 days of shaking was found to be sufficient to ensure equilibrium, an aliquot was filtered using a 0.45 μm filter. The pH of the filtrate was measured. The filtrates were appropriately diluted, when necessary, and the content of Dipy in each solution was determined by measuring the first derivative amplitude at 278 nm. In the thermodynamic study, the same procedure was repeated in 0.05 M citrate buffer (pH 8.7) at 21, 31, 37 and 45 °C.

The PSDs obtained were rigorously analyzed to obtain estimates of complex formation constants ($K_{ij}$) through linear and nonlinear regression analysis, which were discussed earlier [9, 11]. By assuming the formation of 1:1 (SL) and 1:2 ($SL_2$) soluble Dipy/β-CD complexes, the individual formation constants of SL and $SL_2$ complexes defined as $K_{11}$ and $K_{12}$ are given by:

$$K_{11} = \frac{[SL]}{[S][L]} \quad (7)$$

$$K_{12} = \frac{[SL_2]}{[SL][L]} \quad (8)$$

The solubility ($S_{eq}$) of Dipy in aqueous CD solutions of variable concentrations is given by:

$$S_{eq} = S_o + [SL] + [SL_2] = S_o + K_{11}S_o[L] + K_{11}K_{12}S_o[L]^2 \quad (9)$$

where $S_o$ and [L] donate the concentrations of free Dipy and β-CD, respectively, while [SL] and [$SL_2$] represent the concentrations of 1:1 and 1:2 Dipy/β-CD complexes, respectively.

The total concentration of $\beta$-CD in solution ($L_{eq}$) is given by

$$L_{eq} = [L] + [SL] + 2[SL_2] = [L] + K_{11}S_o[L] + 2K_{11}K_{12}S_o[L]^2 \quad (10)$$

To compensate for buffer species/$\beta$-CD complex formation in citrate buffers at pHs < 5, the contribution of citric acid ($H_3A$) and monosodium citrate ($H_2A^-$) to complex formation, which was estimated at complex formation constant ($K_B$) = 15.6 $M^{-1}$ from the variation of $\beta$-CD solubility with the total concentrations of $H_3A$ and $H_2A^-$ ($B_o$) at pHs 2.5, 4.4 was accounted for in the analysis of PSDs [9, 12].

Rigorous nonlinear regression of experimental data was conducted using the Marquardt-Levenberg finite difference algorithm utilized by the SPSS statistical package (SPSS 10.0 for Windows Statistical Package, SPSS Inc., 233 S. Wacker Drive, Chicago, Illinois), and data plots were linked to Microsoft Excel for reproduction.

### Proton nuclear magnetic resonance ($^1$H-NMR)

$^1$H-NMR spectra were obtained at 400 MHz and 25 °C on a spectrometer (GSX400, JEOL/Japan). Samples were dissolved in 99.98% $D_2O$ and filtered before use. Chemical shifts are quoted relative to sodium 3-trimethylsilyl [$D_4$] propionate at 0.0 ppm but spectra were calibrated via the known position of the residual HOD resonance, which was used as an external reference.

### Differential scanning calorimetry (DSC)

The samples were separately put in aluminum pans for thermal analysis. The corresponding thermograms were recorded at a scanning speed of 10 °C/min (910S, TA instrument/USA). The salts and their complexes were dried 2 days at 40 °C prior to analysis.

### X-ray powder diffractometry (XRPD)

The XRPD patterns were measured with x-ray diffractometer (Philips PW 1729 X-Ray Generator, Holland). Radiations generated from Co $K_\alpha$ source and filtered through Ni filters with a wavelength of 1.79025 Å at 40 mA and 35 kV were used. The instrument was operated with a scanning rate of 0.02°/s over the $2\theta$ range of 5–55°.

### Scanning electron microscope (SEM)

The morphology was determined with a scanning electron microscope. The sample (0.5 mg) was mounted onto a 5 × 5 mm silicon wafer affixed via graphite tape to an aluminum stub. The powder was then sputter-coated for 40 s at a beam current of 38–42 mM with a 100 Å layer of gold/palladium alloy.

### Molecular mechanical modeling ($MM^+$)

Molecular mechanical modeling was performed by $MM^+$ force field using HyperChem6 software (Hypercube, Canada) as described earlier [8, 13]. Interaction energies were computed for Dipy approaching from piperidine and diethanolamine groups through the wide and narrow rims of $\beta$-CD cavity. Different 1:1 complex geometries were generated by manual docking of the guest molecule. Then, optimal configurations were obtained by performing geometry optimization for each starting geometry. For the 1:2 complex, the second $\beta$-CD molecule was introduced manually to each of the optimal 1:1 complexes in three different orientations (wide rim–wide rim, wide–narrow, narrow–narrow). The binding energies ($E_{binding} = E_{complex} - \sum E_{components}$) corresponding to energy minima were computed together with their electrostatic ($E_{es}$) and van der Waals ($E_{vdw}$) contributions.

## Results and discussion

### Acid–base ionization ($pK_a$) and solubility product ($pK_{sp}$) constants

Analysis of the variation of the first derivative UV absorptivity of a fixed concentration of Dipy (0.02 mM) at 294 nm with pH (Fig. 2) according to Eq. 3 yielded the $pK_a$ values of 6.4 corresponding to ionization of the

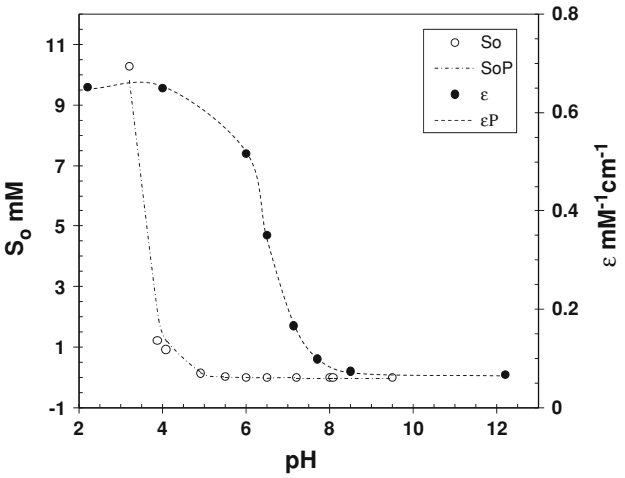


**Fig. 2** Plots of the variation of the 1st derivative UV absorptivity ($\varepsilon$) of a fixed concentration of Dipy (0.02 mM) at 294 nm and the apparent solubility of Dipy ($S_o$) against pH. Both measured in 0.05 M citrate buffer at 30 °C

piperidine moiety. Non-linear regression of the corresponding pH solubility profile (Fig. 2) yielded the two p$K_a$ values of 6.2 and 2.7 corresponding to ionization of piperidine and diethanolamine moieties, respectively. The obtained p$K_a$ value of piperidine moiety by both methods is in agreement with that calculated earlier (p$K_a$ = 6.2) by linear extrapolation using potentiometric titration in mixtures of methanol and water [14]. Dipy does not show salt saturation with the buffer counter ion at low pHs (Fig. 2).

## Interaction of Dipy with $\beta$-CD in solution

### *Phase solubility diagrams (PSDs) and measuring the contribution of the drug hydrophobic character to complex formation*

PSDs of the Dipy/$\beta$-CD system obtained in citrate and phosphate buffers at different pHs and at 30 °C are shown in Fig. 3a and b. The corresponding inherent solubility ($S_o$) and complex formation constants ($K_{11}$ and $K_{12}$) are listed in Table 1. The results indicate that neutral and protonated Dipy species exhibit an $A_L$-type PSDs. The $K_{11}$ values over at all pHs showed no general trend as $S_o$ decreases (e.g., as pH increases). This is rather unexpected if the driving force for inclusion stems solely from the hydrophobic effect [8, 9, 12, 15–17], since $S_o$ at pH = 10.5 ($4.6 \times 10^{-3}$ mM) is much lower than at pH = 4.1 (950 mM). The influence of changing the citrate buffer concentration on the $K_{11}$ values was also investigated (Fig. 3c, Table 1). The same trend was observed where no significant increase in $K_{11}$ value by increasing buffer concentration even the $S_o$ decreases. This again indicated that the hydrophobic character of Dipy does not contribute significantly to complex formation. It is worth mentioning that the $K_{12}$ value increases by increasing citrate buffer concentration as shown in Table 1 (e.g., as $S_o$ decreases). This is clear from the changing of the type of PSDs from $A_L$ to $A_P$ by increasing buffer concentration, which indicates the formation of higher order complex [10].

The extent to which complex formation is influenced by specific interactions and the hydrophobic effect is evaluated from a plot of –RT ln $K_{11}^x$ against −RT ln $S_o^x$ (Fig. 4) from the variation $K_{11}^x$ and $S_o^x$ with pH and buffer concentration at same temperature [8, 9, 12, 15–17]. In Fig. 4, $x$ represents the mole fraction standard state, where the units of $K_{11}$ ($M^{-1}$) and $S_o$ (mM) in Table 1 were transformed into mole fraction units by multiplying $K_{11}$ with 55.5 and dividing $S_o$ by 55.5, respectively (55.5 represents the number of moles of water in 1,000 mL). The plot indicates that the tendency for complex formation is not significantly driven by the hydrophobic character of Dipy, in which the magnitude of the slopes is very small ranging from 0.0 to 6.3%. Other factors including specific

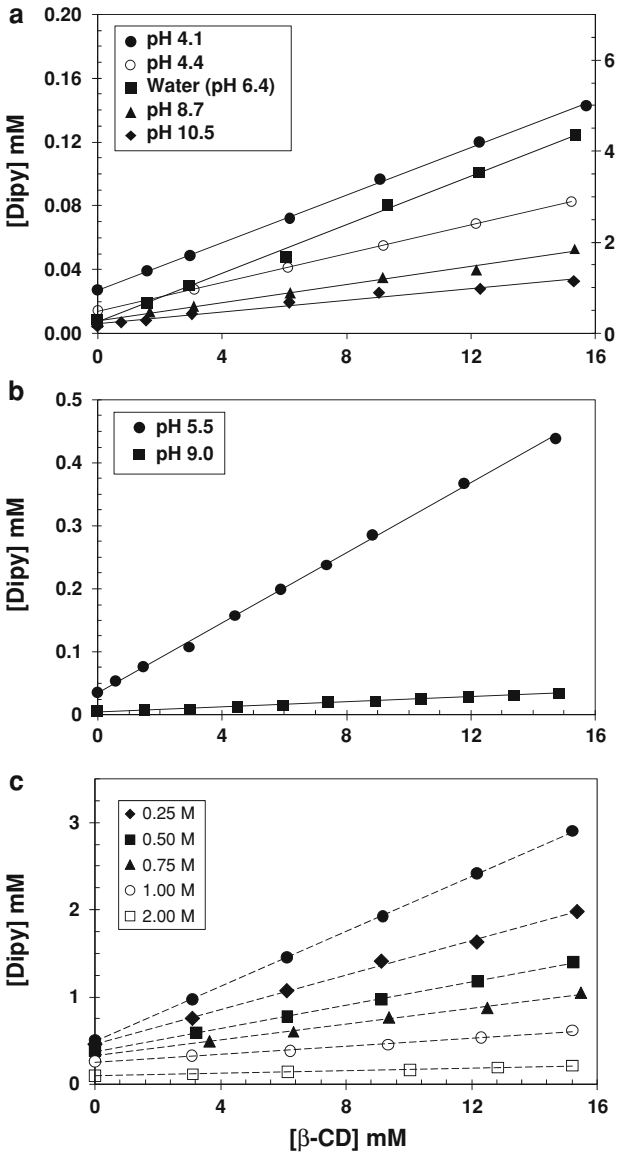


**Fig. 3** Phase solubility diagrams of the Dipy/$\beta$-CD system in (**a**) 0.05 M citrate buffer (**b**) 0.1 M phosphate buffer and (**c**) citrate buffer of different concentrations all at 30 °C, right $y$-axis of Fig. 1a corresponds to pH 4.2

interactions constitute –25 to –26 kJ/mol (intercepts). In previous works [8, 9, 12, 15–17], the contribution of the hydrophobicity of some basic and acidic drugs to complex formation is ranging from 35 to 80%. This indicates that other specific interaction involved in Dipy/$\beta$-CD complex stability rather than the drug hydrophobic character.

### *Thermodynamics*

The PSDs of Dipy obtained in 0.05 M citrate buffer (pH 8.7) at different temperatures are shown in Fig. 5a. The corresponding complex formation constants ($K_{11}$) and the solubilities of Dipy in the absence of $\beta$-CyD ($S_o$) are

**Table 1** Complex formation constants ($K_{11}$ and $K_{12}$) obtained from phase solubility diagrams for the Dipy/$\beta$-CD system in different media and 30 °C

| In 0.05 M citrate buffer of different pHs | | | |
|---|---|---|---|
| pH | $S_o \times 10^3$ (mM) | $K_{11}$ ($M^{-1}$) | $K_{12}$ ($M^{-1}$) |
| 4.1 | 950 (37) | 365 (31) | 1.0 (0.6) |
| 4.4 | 506 (9) | 618 (56) | 9.0 (0.5) |
| 8.7 | 7.0 (1.2) | 290 (52) | 0.3 (0.03) |
| 10.5 | 4.6 (0.8) | 517 (55) | 1.0 (0.3) |
| $H_2O$ (pH 6.4) | 9.0 (2.0) | 716 (177) | 16 (4) |

| In citrate buffer of different concentrations at pH 4.4 | | | | |
|---|---|---|---|---|
| | pH | $S_o \times 10^3$ (mM) | $K_{11}$ ($M^{-1}$) | $K_{12}$ ($M^{-1}$) |
| [Citrate] M | | | | |
| 0.05 | 4.4 | 506 (9) | 618 (56) | 9 (1) |
| 0.25 | | 454 (22) | 799 (59) | 10 (1) |
| 0.50 | | 382 (8) | 960 (33) | 34 (2) |
| 0.75 | | 337 (14) | 841 (62) | 67 (5) |
| 1.00 | | 261 (10) | 565 (48) | 250 (22) |
| 2.00 | | 97 (4) | 859 (83) | 529 (51) |

| In 0.1 M phosphate buffers of different pHs | | | |
|---|---|---|---|
| pH | $S_o \times 10^3$ (mM) | $K_{11}$ ($M^{-1}$) | $K_{12}$ ($M^{-1}$) |
| 5.5 | 35 (2) | 824 (60) | – |
| 9.0 | 4.5 (0.3) | 390 (30) | 11 (1) |

$S_o$ is the inherent Dipy solubility. Numbers in brackets denote absolute errors estimated for a 95% confidence level

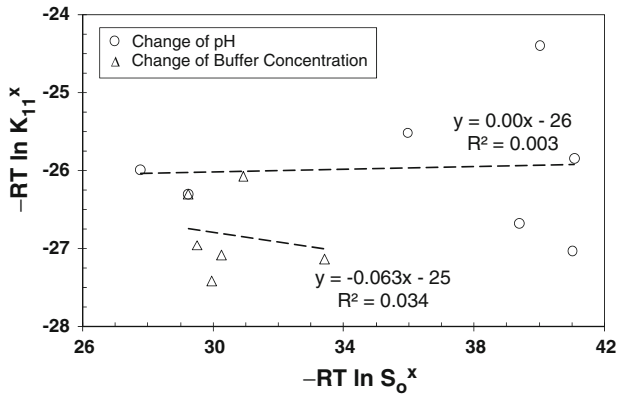


**Fig. 4** Plot of the free energy of 1:1 complex formation (−RT ln $K_{11}^x$) against the free energy of the inherent Dipy solubility (−RT ln $S_o^x$) for the data of Table 1 ($x$ denotes the mole fraction standard state)

listed in Table 2. Van't Hoff plots of ln $K_{11}^x$ and ln $S_o^x$ against 1/T are shown in Fig. 5b, while the thermodynamic parameters ($\Delta H°$, $\Delta S°$ and $\Delta G°$) are listed in Table 2.

The results indicate that complex formation ($\Delta G° = -24.3$ kJ/mol) is favored both by enthalpy ($\Delta H° = -14.8$ kJ/mol) and entropy ($\Delta S° = 31.9$ J/mol.K), which is

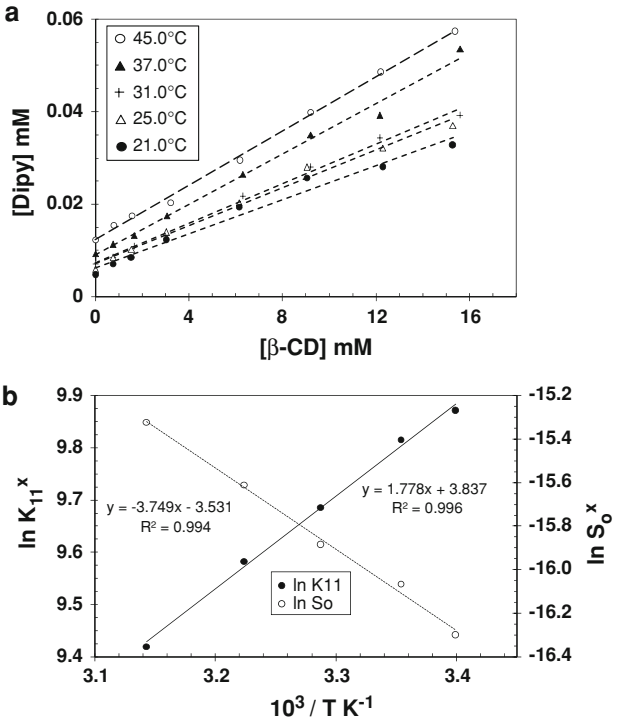


**Fig. 5** **a** Phase solubility diagrams of the Dipy/$\beta$-CD system in 0.05 M citrate buffer (pH 8.7) at different temperatures. **b** Plots of ln $K_{11}^x$ and ln $S_o^x$ against $1/T$ for the data of Table 2

**Table 2** Thermodynamic parameters of the Dipy/$\beta$-CD system in 0.05 M citrate buffer (pH 8.7) obtained from van't Hoff plots

| Temperature (°C) | $S_o \times 10^3$ (mM) | $K_{11}$ ($M^{-1}$) | |
|---|---|---|---|
| 21.0 | 4.6 (0.2) | 348 (43) | |
| 25.0 | 5.8 (0.3) | 330 (50) | |
| 31.0 | 7.0 (0.3) | 290 (33) | |
| 37.0 | 9.2 (0.2) | 261 (17) | |
| 45.0 | 12.3 (0.6) | 222 (42) | |
| | $\Delta G°$ (kJ/mol) | $\Delta H°$ (kJ/mol) | $\Delta S°$ (J/K.mol) |
| 1:1 complex | −24.3 (1.7) | −14.8 (1.7) | 31.9 (5.6) |
| $S_o$ (Solubility) | 39.9 (3.6) | 31.1 (3.6) | −29.5 (12.1) |

Numbers in brackets denote absolute errors estimated for a 95% confidence level

mainly attributed to Van der Waals interactions and solvent disordering, respectively [18]. While Dipy solubility is impeded by both enthalpy ($\Delta H° = 31.1$ kJ/mol) and entropy ($\Delta S° = -29.5$ J/mol.K) changes. The positive enthalpy and negative entropy changes indicate that energy is needed to break the Dipy molecule away from its pure phase, and to separate the water molecules so there is a vacant space or "cavity" for the incoming molecule. The negative effect on entropy indicates that the Dipy molecules are incapable of forming hydrogen bonds with the

water molecules, which causes the water molecules to reestablish some hydrogen bonds by changing their orientation, and this results in a more ordered structure (cage effect). [19]. It is worth mentioning that the experiment dealing with the chemical stability of protonated (at pH 4.0) and neutral Dipy (at pH 9.0) in 0.05 mM citrate buffer at 45 °C was carried out for 2 days. The HPLC analysis indicated that Dipy is stable in the absence and presence of $\beta$-CD without any significant loss in its potency (The assay is ranging from 98.7 to 100.7%).

*Proton nuclear magnetic resonance ($^1$H-NMR)*

$^1$H-NMR spectra of $\beta$-CD, Dipy.HCl salt and their corresponding complex with $\beta$-CD were measured in $D_2O$ at 25 °C (Fig. 6). The results show that the upfield $\Delta\delta$ on complexation are highest for protons $H_3$ (−0.052 ppm) and $H_5$ (−0.086 ppm) of $\beta$-CD. This indicates deep penetration of Dipy into the $\beta$-CD cavity [20], whereas the outer protons $H_1$, $H_2$, $H_4$ and $H_{6,6'}$ demonstrate less $\Delta\delta$ (−0.02 to 0.002 ppm) upon complexation. For the piperidine and diethanolamine groups, all protons showed downfield $\Delta\delta$ (0.018–0.084 ppm). The displacement is higher for piperidine compared with those for the diethanolamine indicating that the piperidine groups might be more exposed to the hydroxyls of $\beta$-CD in the 1:2 type Dipy/$\beta$-CD complexes formed. This might explains the formation of relatively strong complexes of protonated Dipy with $\beta$-CD although of its high solubility. At the acidic pH values studied in this work, the protonation occurs for the nitrogen in the piperidine ring ($pK_a = 6.4$) thus with the assumption that more or less similar complex geometries

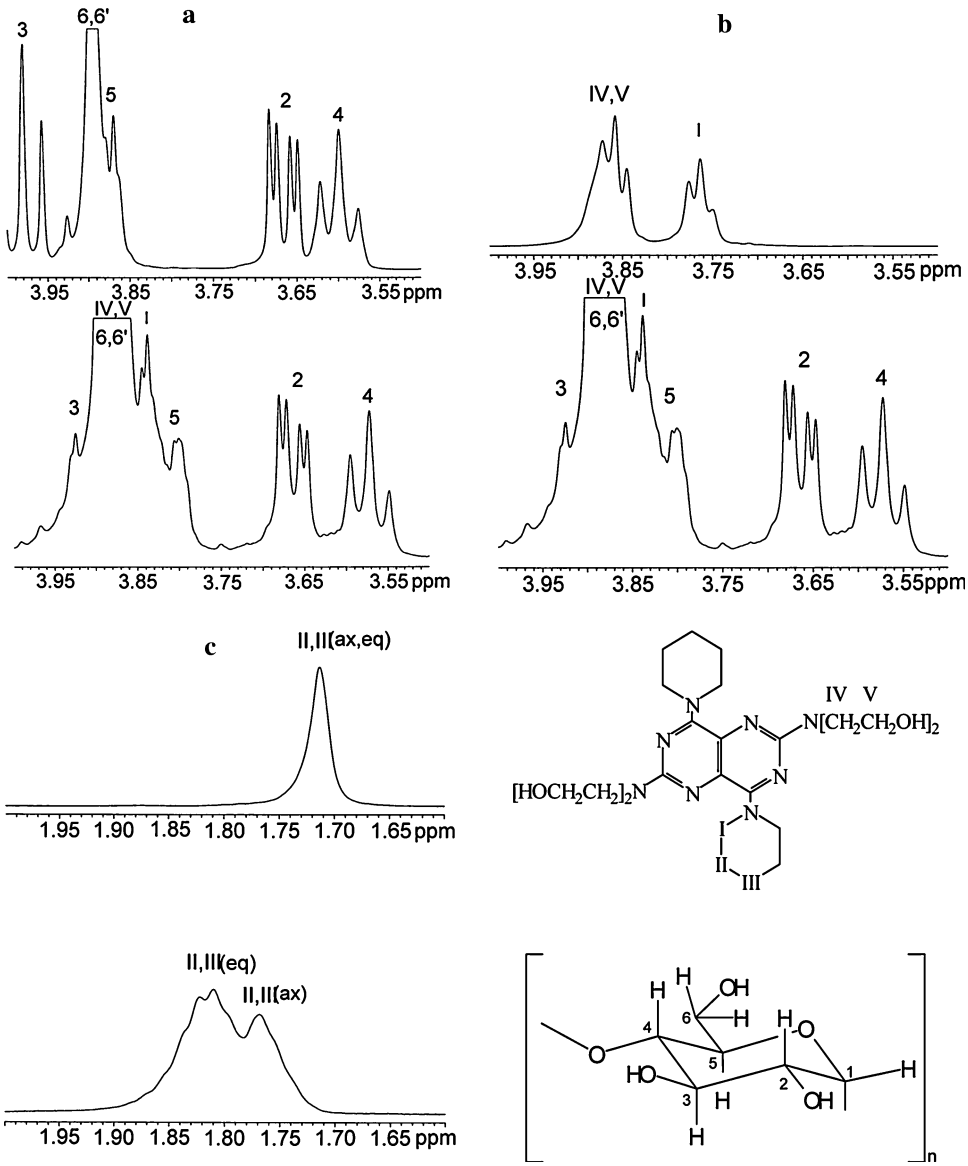


**Fig. 6** $^1$H-Nuclear magnetic resonance spectra of the Dipy.HCl/$\beta$-CD system in $D_2O$ at 25 °C (**a**) for protons of $\beta$-CD and (**b**) and (**c**) for protons of Dipy.HCl. The upper and lower traces correspond to the compound before and after complexation, respectively

for the neutral and protonated Dipy/β-CD complexes, the piperidine group interacts via ion-dipole interactions with the hydroxyl groups of β-CD explaining the strong binding of the protonated species similar to the neutral Dipy (Table 1).

## Characterization of Dipy.HCl/β-CD solid complex

### *Powder x-ray diffractometry (PXD)*

The XRPD patterns of Dipy.HCl, β-CD, physical mixture of 1:2 Dipy.HCl and β-CD, and their corresponding complex are presented in Fig. 7. It is clear that the XRPD pattern of the physical mixture of Dipy.HCl and β-CD (Fig. 7c) is almost superposition of the patterns contributed by Dipy.HCl and β-CD (Fig. 7a, b). The dominant of the principal peaks of β-CD in the physical mixture is a result of its high percentage in the mixture (82% w/w). In contrast, the diffraction pattern of Dipy.HCl/β-CD complex (Fig. 7d) showed complete disappearance of principal diffraction peaks apparent in the XRPD patterns of Dipy.HCl and β-CD, which suggests the formation of an inclusion complex with a new solid phase.

### *Differential scanning calorimetry (DSC)*

Figure 8 shows the thermal behaviors of all samples of Dipy.HCl, a physical mixture of 1:2 Dipy.HCl and β-CD, and the isolated 1:2 Dipy.HCl/β-CD solid complex. Dipy.HCl has an endothermic peak at about 170 °C (Fig. 8a), which retained in the physical mixture of Dipy.HCl and β-CD (Fig. 8c), but disappeared in the thermogram of the complex (Fig. 8d) indicating that Dipy.HCl forms an inclusion complex with β-CD.

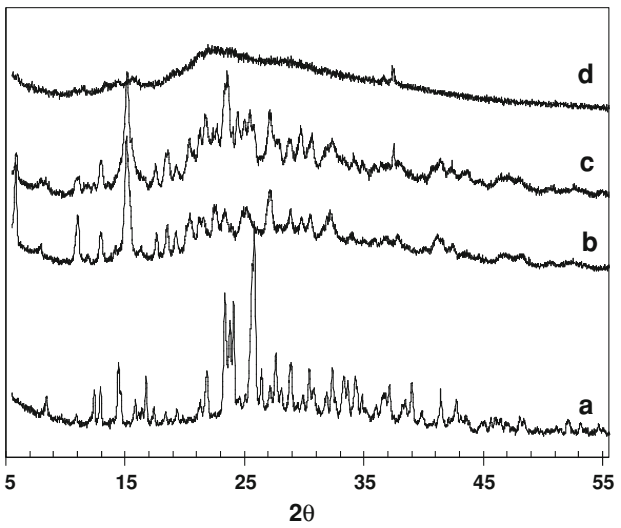


**Fig. 7** X-ray powder diffraction patterns of (**a**) Dipy.HCl, (**b**) β-CD, (**c**) a physical mixture of 1:2 Dipy.HCl and β-CD and (**d**) 1:2 Dipy.HCl/β-CD complex

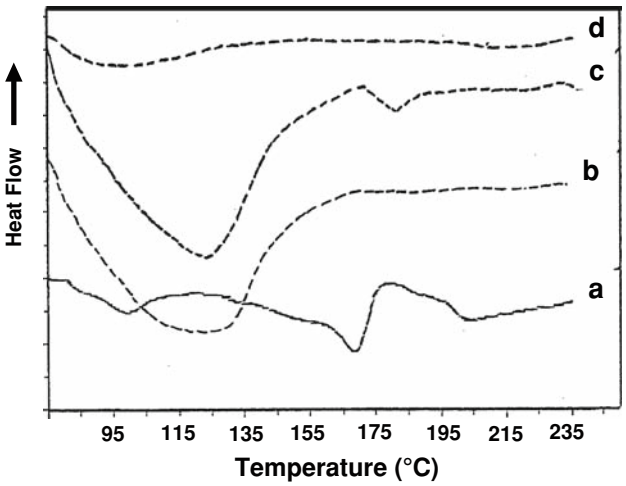


**Fig. 8** Differential scanning calorimetric thermograms of (**a**) Dipy.HCl, (**b**) β-CD, (**c**) a physical mixture of 1:2 Dipy.HCl and β-CD and (**d**) 1:2 Dipy.HCl/β-CD complex

### *Scanning electron microscopy (SEM)*

Figure 9a, b and c present the SEM images of Dipy.HCl, β-CD and it corresponding 1:2 physical mixture, respectively. In the physical mixture (Fig. 9c), the morphology of both compounds is maintained with the dominant of β-CD particles. In contrast the SEM images of the freeze-dried Dipy.HCl/β-CD system (Fig. 9d) showed that it is impossible to differentiate between the two components indicating the best interaction of Dipy.HCl particles with β-CD. The obtained images support the idea of the consecution of a homogeneous crystal mass (Fig. 9d). Thus, the SEM result, along with the results of XRPD and DSC studies, confirm the inclusion complex.

## Molecular mechanical modeling ($MM^+$) and optimal complex configurations

Molecular modeling of the Dipy/β-CD interaction was conducted for the four different approaches of the piperidine and diethanolamine sides through the wide and narrow rims of β-CD. The corresponding binding energies ($E_{binding}$) are listed in Table 3. The result indicate that both piperidine and diethanolamine moieties ($E_{binding} = -176$ and $-173$ kJ/mol, respectively) are almost equally included (Fig. 10a ,b). In the 1:2 Dipy/β-CD inclusion complex, inclusion of both piperidines $E_{binding} = -288$ kJ/mol) is only slightly more probable than diethanolamine ($E_{binding} = -280$ kJ/mol) moieties (Fig. 10c ,d). Thus both $^1$H-NMR and $MM^+$ studies indicate the formation of isomeric 1:1 and 1:2 complexes [8, 15–17]. It was reported earlier that the Van

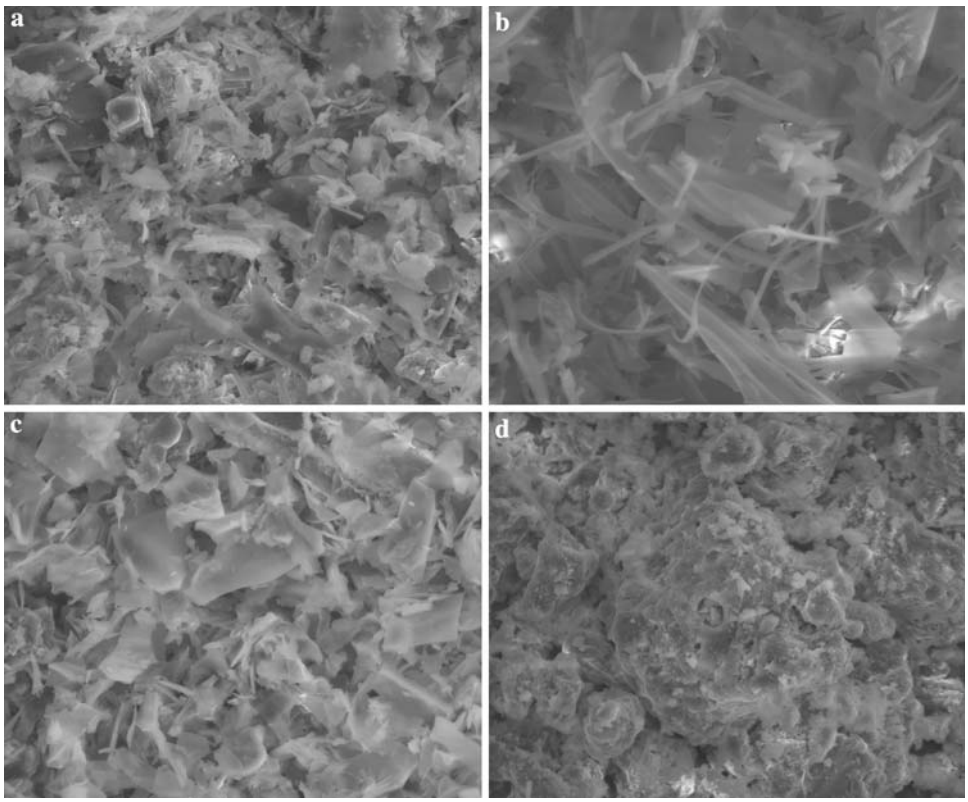


**Fig. 9** Scanning electron microscope images of (**a**) Dipy.HCl, (**b**) $\beta$-CD, (**c**) a physical mixture of 1:2 Dipy.HCl and $\beta$-CD and (**d**) 1:2 Dipy.HCl/$\beta$-CD complex

**Table 3** Molecular modeling results of the interaction energies (kJ/mol) corresponding to optimal configurations of the Dipy/$\beta$-CD inclusion complexes (1:1 and 1:2) obtained at different approaches

| Approach/Moieties included | $E_{binding}$ | $E_{vdw}$ | $E_{electrostatic}$ |
|---|---|---|---|
| 1:1 complex | | | |
| Diethanolamine NR/Diethanilamine | −176 | −135 | −41 |
| Piperidyl WR/Piperidine | −173 | −141 | −32 |
| 1:2 complex | | | |
| Piperidyl WR-Piperidyl WR/The two piperdine groups | −288 | −236 | −52 |
| Diethanolamine WR-Diethanolamine WR/The two diethanolamine groups | −280 | −242 | −38 |

der Waals forces have the major contribution to complex stability, with minor contribution from the electrostatic interactions [8, 15–17]. In the present work, the results in Table 3 reveal that the major contribution to the complex stability also arises from Van der Waals interactions; but there is a significant contribution from the electrostatic interactions indicating the importance of dipole–dipole forces in this system.

## Conclusion

Neutral and ionized Dipy have nearly the same tendency toward complex formation. This indicates that the hydrophobic character of Dipy does not significantly contribute to complex formation (0.0 to 6.3%). This result does not in agreement with what was reported for some basic and acidic drugs to complex formation, where the contribution of the hydrophobicity is ranging from 35 to 80%. This indicates that other specific interaction involved in Dipy/$\beta$-CD complex stability rather than the drug hydrophobic character. Complex formation of the neutral Dipy with $\beta$-CD ($\Delta G°$=−24.3 kJ/mol) is driven by both favorable enthalpy ($\Delta H°$=−14.8 kJ/mol) and entropy ($\Delta S°$= 31.9 J/mol.K) changes. Phase solubility, $^1$H-NMR, and $MM^+$ studies indicate the formation of isomeric 1:1 and 1:2 complexes, where both piperidine and diethanolamine moieties are involved in inclusion complexation. All the data obtained

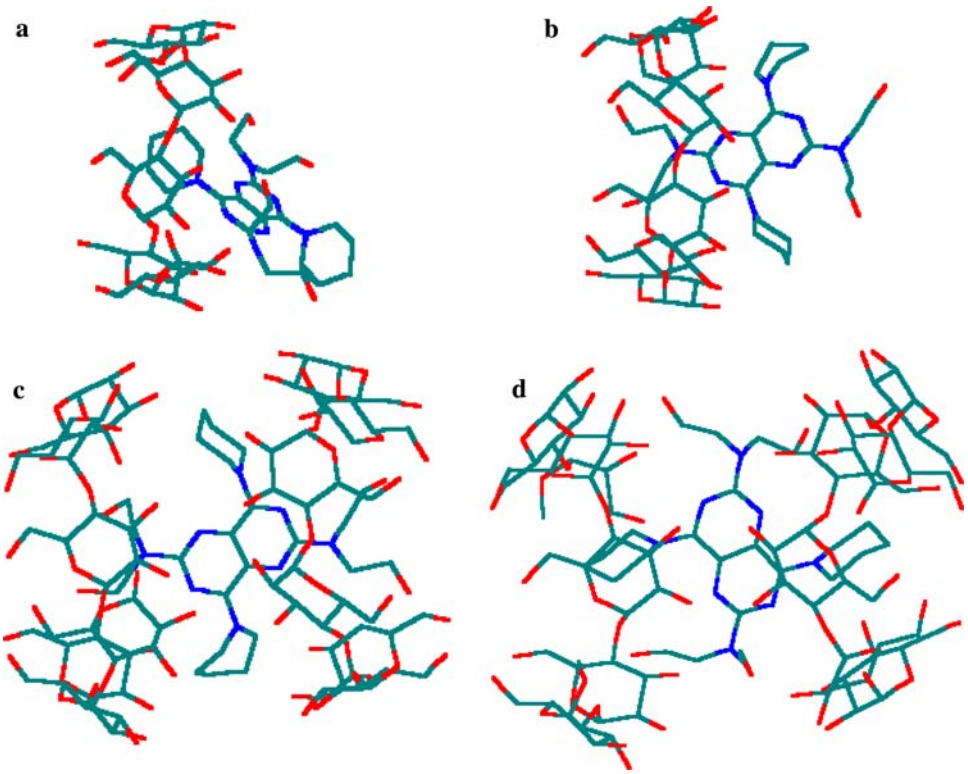


**Fig. 10** Side views of the most probable Dipy/$\beta$-CD configurations obtained for the 1:1 complex for the inclusion of (**a**) piperidine and (**b**) diethanolamine moieties and for the inclusion of (**c**) both diethanolamine and (**d**) both piperidine moieties for the 1:2 complexes. In all figures, part of one glucose unit of the $\beta$-CD molecules was removed for clarification

from the Phase solubility, $^1$HNMR, XRPD, DSC, and SEM indicate the formation of true inclusion complex between Dipy and $\beta$-CD in solution and in the solid state.

## References


1. AHFS drug information: Dipyridamole monograph. www.ashp.Org/mngrphs/ahfs/a382830.htm
2. Drug bank: Dipyridamole monograph. http://www.drugbank.ca/drugs/DB00975
3. Khalil, A., Belal, F., Al-Badr, A.A.: Dipyridamole comprehensive profile. In: Brittain, H.G. (ed.) Profiles of Drug Substances, Excipients, and Related Methodology, vol. 31, pp. 215–280. Elsevier Academic Press Inc., CA/USA (2005)
4. Stella, V.J., Rajewski, R.A.: Cyclodextrins: their future in drug formulation and delivery. Pharm. Res **14**, 556–567 (1997). doi:10.1023/A:1012136608249
5. Del Valle, E.M.M.: Cyclodextrins and their uses: a review. Process Biochem **39**, 1033–1046 (2004). doi:10.1016/S0032-9592(03)00258-9
6. Loftsson, T., Duchêne, D.: Cyclodextrins and their therapeutic applications. Int. J. Pharm. **329**, 1–11 (2007). doi:10.1016/j.ijpharm.2006.10.044
7. Torri, G., Naggi, A., Fregnan, G.B., Trebbi, A.: Dipyridamole-$\beta$-cyclodextrin complex: preparation and characterization. Pharmazie **45**, 193–195 (1990)
8. Al Omari, M.M., Zughul, M.B., Davies, J.E.D., Badwan, A.A.: Sildenafil/cyclodextrin complexation: stability constants, thermodynamics, and guest-host interactions probed by $^1$H-NMR and molecular modeling studies. J. Pharm. Biomed. Anal **41**, 857–865 (2006). doi:10.1016/j.jpba.2006.01.055
9. Al Omari, M.M., Zughul, M.B., Davies, J.E.D., Badwan, A.A.: Effect of buffer species on the complexation of basic drug terfenadine with $\beta$-cyclodextrin. J. Incl. Phenom. Macrocycl. Chem **58**, 227–235 (2007). doi:10.1007/s10847-006-9147-5
10. Higuchi, T., Connors, K.A.: In: Reilley, C.N. (ed.) Advances in Analytical Chemistry Instrumentation, pp. 117–212. Wiley-Interscience, New York (1965)
11. Zughul, M.B., Badwan, A.A.: $SL_2$ type phase solubility diagrams, complex formation and chemical speciation of soluble species. J. Incl. Phenom. Macrocycl. Chem **31**, 243–264 (1998). doi:10.1023/A:1007965424219
12. Al Omari, M.M., Zughul, M.B., Davies, J.E.D., Badwan, A.A.: Effect of buffer species on the inclusion complexation of acidic drug celecoxib with cyclodextrin in solution. J. Incl. Phenom. Macrocycl. Chem **55**, 247–254 (2006). doi:10.1007/s10847-005-9041-6
13. Taraszewska, J., Migut, K., Kozbiat, M.: Complexation of flutamide by native and modified cyclodextrins. J. Phys. Org. Chem **16**, 121–126 (2003). doi:10.1002/poc.582
14. Avdeef, A., Bendels, S., Tsinman, O., Tsinman, K., Kansy, M.: Solubility-excipient classification gradient maps. Pharm. Res **24**, 530–545 (2007). doi:10.1007/s11095-006-9169-0
15. Al Omari, M.M., Zughul, M.B., Davies, J.E.D., Badwan, A.A.: Cisapride/$\beta$-cyclodextrin complexation: stability constants, thermodynamics, and guest-host interactions probed by $^1$H-NMR and molecular modeling studies. J. Incl. Phenom. Macrocycl. Chem **57**, 511–517 (2007). doi:10.1007/s10847-006-9242-7
16. Al Omari, M.M., El-Barghouthi, M.I., Zughul, M.B., Davies, J.E.D., Badwan, A.A.: Comparative study of the inclusion complexation of pizotifen and ketotifen with native and modified

cyclodextrins. J. Solut. Chem **37**, 249–264 (2008). doi:10.1007/s10953-007-9234-2
17. Al Omari, M.M., Zughul, M.B., Davies, J.E.D., Badwan, A.A.: Astemizole/cyclodextrin inclusion complexes: phase solubility, physicochemical characterization and molecular modeling studies. J. Solut. Chem **37**, 875–893 (2008). doi:10.1007/s10953-008-9277-z
18. Ventura, C.A., Giannone, I., Paolino, D., Pistara, V., Corsaro, A., Puglisi, G.: Preparation of celecoxib-dimethy-$\beta$-cyclodextrin inclusion complex: characterization and in vitro permeation study. Eur. J. Med. Chem **40**, 624–631 (2005). doi:10.1016/j.ejmech.2005.03.001
19. Saichek, R.E., Reddy, K.R.: Electrokinetically enhanced remediation of hydrophobic organic compounds in soils: a review. Crit. Rev. Environ. Sci. Technol **35**, 115–192 (2005). doi:10.1080/10643380590900237
20. Connors, K.A.: The stability of cyclodextrin complexes in solution. Chem. Rev **97**, 1325–1358 (1997). doi:10.1021/cr960371r